BioMed

MDPI

Article

Neuroimaging-Based Brain Morphometry in Alzheimer's Disease

Nonyelum Aniebo [1] and Tarun Goswami [2,*]

[1] Department of Biomedical, Industrial and Human Factors Engineering, Wright State University, Dayton, OH 45435, USA; aniebo.2@wright.edu
[2] Department of Orthopedic Surgery, Sports Medicine and Rehabilitation, Miami Valley Hospital, Dayton, OH 45409, USA
* Correspondence: tarun.goswami@wright.edu

Abstract: Background/Objectives: Alzheimer's disease (AD) is a leading cause of death worldwide, affecting millions of older Americans and resulting in a substantial economic burden. The Alzheimer's Disease Neuroimaging Initiative (ADNI) aims to investigate and develop treatments for AD. **Methods:** This study included 60 participants, divided equally into AD and control cohorts, and utilized magnetic resonance imaging (MRI) scans to detect gray matter volumetric alterations, a key biomarker of AD. The participants' cortical volume and surface area were quantified using an automated pipeline in MIMICS (Materialise Interactive Medical Imaging Control System). **Results:** A multivariate regression analysis was conducted to explore the relationship between cortical measurements and potential factors influencing AD susceptibility. The study found that both cortical volume and surface area were statistically significant predictors of AD ($p = 0.0004$ and $p = 0.011$, respectively). Age was also a significant factor, with the 65–70 age group showing the strongest association ($p < 0.001$). The model achieved an accuracy of 0.68 in predicting AD. **Conclusions:** While voxel-based morphometry (VBM) using MIMICS showed promise, further development of the automated pipeline could enhance accuracy and correlation indices. These findings contribute to our understanding of brain atrophy in AD pathophysiology and highlight the potential of MRI morphometry as a tool for AD biomarker development.

Keywords: Alzheimer's disease (AD); magnetic resonance imaging (MRI); gray matter volumetric alterations; cortical volume; neuroimaging

Citation: Aniebo, N.; Goswami, T. Neuroimaging-Based Brain Morphometry in Alzheimer's Disease. *BioMed* **2024**, *4*, 430–445. https://doi.org/10.3390/biomed4040034

Academic Editor: Wolfgang Graier

Received: 29 July 2024
Revised: 4 October 2024
Accepted: 9 October 2024
Published: 17 October 2024

1. Introduction

Alzheimer's disease (AD) is a devastating neurodegenerative disorder characterized by progressive memory loss, cognitive decline, and behavioral changes. As the leading cause of dementia, AD imposes a significant burden on patients, families, and healthcare systems worldwide. The prevalence of Alzheimer's is anticipated to rise sharply due to the global aging population, making it a critical public health concern [1–3]. Current projections estimate that by 2050, the number of individuals living with Alzheimer's disease could triple, further emphasizing the need for early detection and intervention strategies.

At the core of Alzheimer's pathology is neuronal degeneration, which manifests as brain atrophy. Post-mortem studies have consistently identified widespread neuronal loss, particularly in regions associated with memory and cognition, such as the hippocampus and cortex. Importantly, while clinical symptoms may appear gradually, research suggests that neurodegenerative changes begin decades before the first signs of cognitive impairment [4–7]. This pre-symptomatic phase represents a critical window for intervention, underscoring the importance of developing biomarkers that can detect Alzheimer's disease early [8], ideally before irreversible damage occurs.

Among the earliest and most significant changes in the brain of an AD patient is the loss of gray matter, which encompasses regions of the brain responsible for critical functions

such as memory, decision-making, and sensory perception. Consequently, the accurate quantification of gray matter atrophy has the potential to serve as a valuable biomarker for AD [9]. The development of non-invasive, reliable, and cost-effective imaging techniques that can detect gray matter loss in the early stages of the disease is therefore of paramount importance for improving diagnosis, monitoring disease progression, and evaluating treatment efficacy.

Neuroimaging, particularly magnetic resonance imaging (MRI), has emerged as a powerful tool in Alzheimer's research, offering the ability to visualize and quantify structural changes in the brain. Numerous studies have explored automated techniques for analyzing structural T1-weighted MRI images to detect AD-related changes [10,11]. These include established methods such as Statistical Parametric Mapping (SPM), FreeSurfer, FSL-FAST, Advanced Normalization Tools (ANTs), and MALPEM. These methods have demonstrated heterogenous outcomes even with the same subject [12–14]. However, to the best of our knowledge, none have utilized the MIMICS (Materialise Interactive Medical Imaging Control System) software for automatic segmentation of cortical thickness. Consequently, it is crucial to validate the reliability of MIMICS (Materialise Interactive Medical Imaging Control System) for volumetric assessment of gray matter, serving as an outcome measure in Alzheimer's disease clinical trials.

MIMICS 25.0.0.550 manufactured in Leuven, Belgium in Jun 2022 was used for this work. Its robust image processing capabilities and adaptability make it a promising tool for neuroimaging analysis, particularly in the context of AD research.

This study aims to leverage the capabilities of the MIMICS software to develop a novel model of brain morphometry, focusing on the quantification of gray matter atrophy in Alzheimer's disease patients and cognitively normal controls. This research seeks to assess the software's effectiveness in segmenting and analyzing brain structures. The primary objective is to determine whether MIMICS can be a reliable tool for detecting gray matter atrophy and to what extent, which could, in turn, serve as a biomarker for early Alzheimer's detection. Furthermore, this study will perform rigorous statistical validation of the model to evaluate its potential utility in clinical trials and research settings. Through this research, we aim to contribute to the growing body of knowledge in Alzheimer's biomarker development and pave the way for future studies that can enhance the early detection and management of this disease. The analysis showed that part volume and weight were statistically significant factors in predicting Alzheimer's risk, with age being a major risk factor as well. We would like to hypothesize that MIMICS could a reliable tool, in addition to other methods, in predicting the progression of AD.

2. Materials and Method

The secondary data were obtained from Alzheimer's Disease Neuroimaging Initiative (https://adni.loni.usc.edu), It was accessed 1 August 2022 and It's accessible to the public, it does not require additional IRB or consent. For this study, MRI DICOM image files were imported into MIMICS as the first step in the morphometric analysis pipeline (Figure 1) The software enables the visualization and processing of images, enhancing low-quality data by performing noise reduction through cropping and applying digital filters (Figure 2). A discrete Gaussian filter with a 3 mm variance and a maximum kernel size of 3 mm was utilized to smooth and reduce image detail while preserving edges (Figure 3).

Following the filtering, global threshold segmentation was applied (Figures 4 and 5) This method converts grayscale images into binary images based on predefined tissue pixel values, identified using adaptive thresholding (Figure 6). The segmentation process was guided by histogram analysis (Figures 7 and 8), which provided insight into intensity variations, allowing for accurate tissue differentiation. The segmented regions of interest were then used to quantify brain morphology, focusing on cortical atrophy in Alzheimer's disease (AD) patients compared to cognitively normal (CN) controls.

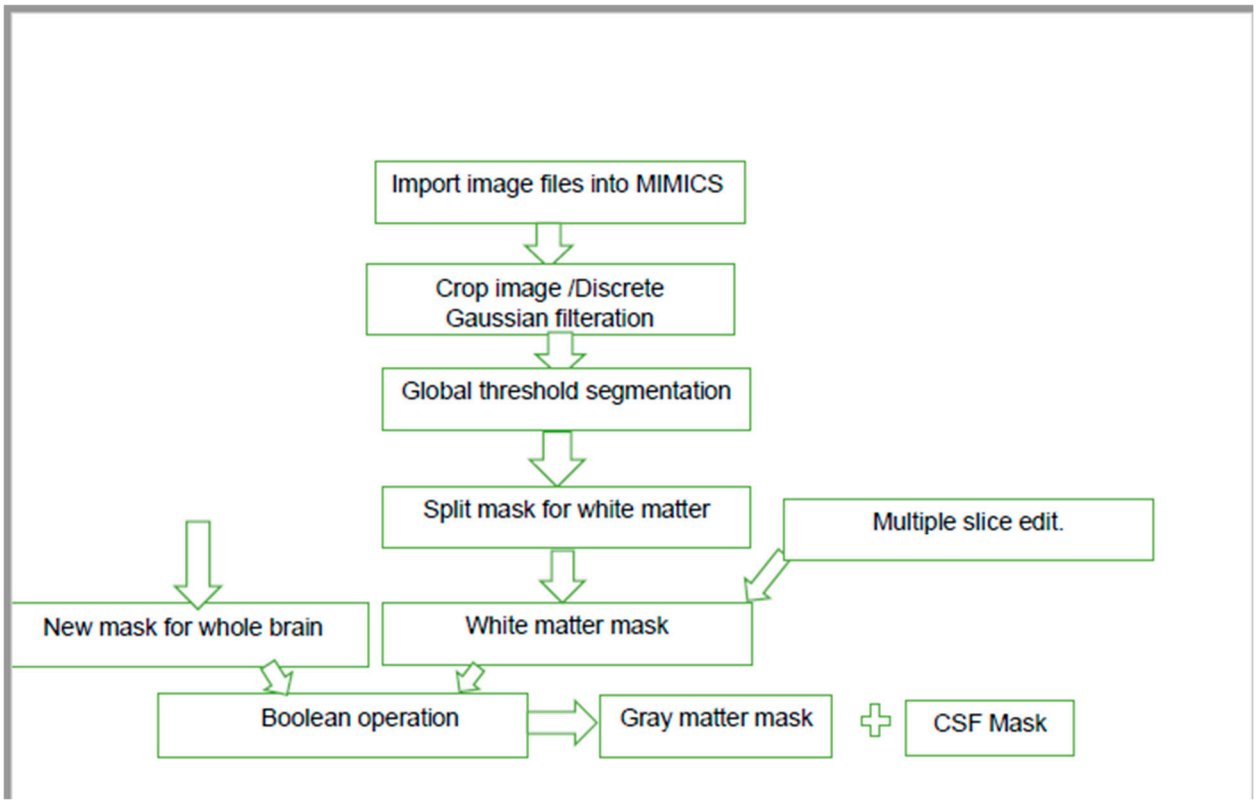

Figure 1. Workflow pipeline developed in MIMICS: a comprehensive overview of the design and implementation process.

2.1. Participants and Rationale

The study utilized data from the Alzheimer's Disease Neuroimaging Initiative (ADNI) database. A total of 60 participants, comprising 30 AD patients and 30 CN subjects, were retrospectively selected from the ADNI 1 study cohort. Participants' ages ranged from 60.1 to 87.9 years, with the AD group aged between 62.2 and 87.9 years and the CN group aged between 60.1 and 87.4 years.

Participants were classified according to ADNI's Alzheimer's disease assessment criteria. CN subjects had no memory complaints, normal memory function based on the Wechsler Memory Scale, a Mini-Mental State Examination (MMSE) score of 24 or above, and a Clinical Dementia Rating (CDR) of 0. AD patients were classified based on memory complaints, abnormal memory function, an MMSE score of 24 or below, and a CDR of 0.5 or greater.

To assess AD progression, participants were evaluated using the Neuropsychiatric Inventory-Questionnaire (NPI-Q) and the Functional Activities Questionnaire (FAQ). The NPI-Q measures neuropsychiatric symptoms, while the FAQ assesses functional impairment in daily activities. The NPI-Q consists of 12 domains, each rated on a 3-point severity scale and a 5-point caregiver distress scale. The FAQ assesses the ability to perform activities of daily living, with a total score ranging from 0 (mild impairment) to 30 (severe impairment).

The MRI data used in this study were acquired during baseline assessments, following an initial screening with a 1.5T MRI scanner. Participants who met the inclusion criteria received a 3T scan at their baseline visit.

2.2. Image Data and Preprocessing

The study exclusively used T1-weighted MR images for morphometric analysis. The original files from the ADNI 1 database consisted of 3D-T1 Magnetization Prepared-Rapid

Gradient Echo (MPRAGE) images from three major MRI vendors: Philips, General Electric (GE) Medicals, and Siemens systems.

To ensure standardization across the images, several preprocessing steps were applied, including gradient warp correction, B1 non-uniformity correction, and N3 intensity normalization. The N3 correction technique, a peak sharpening algorithm, was used to mitigate non-uniform intensity artifacts caused by dielectric effects in high field strength MRI systems.

2.3. Data Analysis and Statistical Approach

The primary focus of the analysis was to investigate cortical atrophy in AD patients compared to CN subjects (Figure 9). Morphometric measurements, including cortical volume and surface area, were extracted from segmented brain images using MIMICS. These parameters were statistically analyzed to determine their relationship with demographic factors, including age, sex, and AD status (Figure 10).

A multivariate regression analysis was conducted to assess the association between cortical atrophy and AD diagnosis, controlling for age and sex. Statistical significance was set at $p < 0.05$. The results were validated using cross-validation techniques, and performance metrics such as accuracy, sensitivity, and specificity were calculated to evaluate the model's predictive capability.

3. Results and Discussion

Only T1-weighted MR images were used to perform the morphometric analyses. All MRI images were original files of ADNI 1 consisting of 3D-T1 Magnetization Prepared Rapid Gradient Echo (MPRAGE) from three major vendors, Philips, General Electrical (GE) Medicals, and Siemens Systems, who had a screening visit and were included for baseline investigation for structural MRI. The sample included 24 males (40%) and 36 females (60%) with a mean age of 73.92 and a standard deviation of 6.39 (Table 1). The age distribution had a range from 60.1 to 87.9 years. While the modal age for the sample under study occurred between 70.1 and 72.1, the least represented age group was between 82.1 and 84.1. Following the 3D voxel calculations from MIMICS, the part volume and surface area measurements of each image file were obtained (Table 2).

Table 1. Summary of bivariate statistical analysis for study participants (N = 60).

All Participants N Variable = 60		CN N = 30 (50%)	AD N = 30 (50%)	p Value
Age	73.92 (6.39)	74.50 (5.97)	73.35 (6.84)	
Weight	67.15 (12.39)	69.09 (9.98)	65 20 (14.32)	
Sex	24 (400%)	11 (36 7%)	13 (43.3%) 17 (56	
Male	36 (60 0%)	19 (63.3%)	7%) 12 20 (5)	0.3
Female	6.12 (7.34)	003 (0.18)	2.60 (2.43)	0.6
FAQ.Total.Score	1.38 (2.13)	0.17 (0.53)	844,474.97	0.2
NPI-	647,778.54	451,082.10	(1,299,250.80)	
Q.Tota1.Score	(940,411.38)	(176,473.57)	313,343.50	
Part.Volume	313,609.83	313,876.16		
Part. SA	(83 928.08)			

The research aims to investigate the differences in brain morphometric analysis between individuals with Alzheimer's disease and healthy controls, utilizing the MIMICS software. It intends to determine whether these morphometric brain measurements can reliably predict the advancement of Alzheimer's disease and to explore whether there is a connection between alterations in brain morphology detected by the MIMICS software and cognitive decline [15].

Table 2. Profile of subjects showing brain part volume and surface area measurements as analyzed using MIMICS.

Subject ID	Sex	Weight	Research Group	Age	FAQ Total Score	NPI-Q Total Score	Part Volume	Part SA
133_S_5250	F	71.1	CN	70.3	0	0	472995.5	266422.4
133_S_0625	F	71.1	CN	70.2	0	0	472995.5	266422.4
133_S_0525	F	71.2	CN	70.3	0	0	472995.5	266422.4
133_S_0493	M	83.9	CN	77.7	0	0	560657.9	348833.4
133_S_0488	F	59.9	CN	71	0	2	51884.9	288597.2
133_S_0433	F	54.2	CN	85.6	0	0	490143.8	283828.6
133_S_0388	F	59.8	CN	71.2	0	2	51884.9	288597.2
116_S_7840	M	73.4	AD	76.6	12	0	564471.2	322660.9
116_S_6472	F	63.7	CN	75.7	0	0	565909.4	329716.9
116_S_6298	F	63.6	CN	75	0	0	575808.4	329610.7
116_S_2930	F	54	AD	84.7	16	7	534701.1	289807.7
116_S_0488	M	73.4	AD	76.7	12	0	564470.2	322660.9
116_S_0487	M	73.4	AD	76.7	12	0	564470.2	322660.9
116_S_0478	M	73.4	AD	76.6	12	0	564471.2	322661.9
116_S_0392	F	54	AD	84.8	16	7	534701.1	289807.7
116_S_0382	F	63.7	CN	75.7	0	0	565807.4	329616.9
116_S_0283	F	63.8	CN	75.8	0	0	565808.4	329616.9
082_S_0640	F	65.2	CN	73.1	0	0	424787.4	309182.8
082_S_0640	F	65.2	CN	73.1	0	0	424787.4	309182.8
082_S_0304	F	65	CN	70.9	0	0	587293.3	371284.8
067_S_5811	M	71.5	AD	62.2	22	7	287200.2	351361.4
067_S_1253	F	62.1	AD	62.8	9	2	511538.8	263384.2
067_S_1185	M	71.6	AD	62.2	22	7	287200.2	351361.4
067_S_0812	F	94.8	AD	71.8	15	3	597952.1	346114.4
037_S_0303	M	59.1	CN	84.4	1	0	525824.5	292879.5
033_S_1610	F	55.7	CN	78.4	0	0	479354.1	264814.1
033_S_1016	F	55.8	CN	78.5	0	0	479353.1	264814.1
033_S_0920	F	59.2	CN	80.2	0	0	480647.5	274192.7
033_S_0724	M	70.8	AD	78.7	18	1	564442.2	358389.4
033_S_0209	F	59.1	CN	80.3	0	0	480647.6	274192.7
032_S_1101	F	37.2	AD	71.2	17	1	496938.7	272852.1
032_S_1011	F	37.2	AD	71.2	17	1	496938.7	272852.1
032_S_0677	M	88.4	CN	71.2	0	0	475764.1	327086.4
031_S_1290	F	64	AD	72.1	8	1	664496.3	360764.4
031_S_1209	F	64	AD	72.1	8	1	664496.3	360764.4
027_S_2801	F	57.9	AD	69.5	18	2	554282.5	301657.6
027_S_1385	F	51.7	AD	69.6	12	7	495933.3	270792.9
027_S_1082	F	57.9	AD	69.6	18	2	554282.5	301657.6
027_S_0407	M	76.3	CN	76.2	0	0	667724.4	331746.6
027_S_0404	F	63.5	AD	87.9	22	0	489884.3	259348.9
027_S_0403	M	76.4	CN	76.4	0	0	667724.4	331746.6
023_S_1690	M	71.7	AD	79.8	0	2	401698.2	447954
023_S_1289	F	47.2	AD	77.5	10	5	360884.8	296039.7
023_S_1262	F	45.8	AD	72.8	7	2	315101.9	317383.7
023_S_0963	M	62.6	CN	72.7	0	0	42264.5	338740.3
023_S_0926	F	75.8	CN	71.3	0	1	419256.1	274074.7
023_S_0916	M	71.7	AD	79.8	0	2	401699.2	447954
023_S_0139	F	60.7	AD	66	10	2	626842	300384
023_S_0061	F	84	CN	77.3	0	0	327895.9	414168.5
023_S_0058	M	71.4	CN	70.2	0	0	38048.06	484656.7
021_S_3570	M	68.8	AD	65.7	7	2	5610393	58361.39
021_S_0753	M	68.9	AD	65.7	7	2	5610393	58361.39
020_S_8821	M	81.6	CN	60.1	0	0	575505.5	355202
020_S_1288	M	81.7	CN	60.1	0	0	575505.5	355202
018_S_0633	M	86.2	AD	83.5	12	0	442909.8	462804.6
018_S_0425	M	82.6	CN	86	0	0	506594	46857.84
018_S_0369	M	81.7	CN	76.2	0	0	506594	468574.8
002_S_1810	F	64.1	AD	70.8	7	3	499229	280779.6
002_S_1018	F	64.1	AD	70.8	7	3	499229	280779.6
002_S_0816	M	101.1	AD	71	13	6	572997.6	507942.1

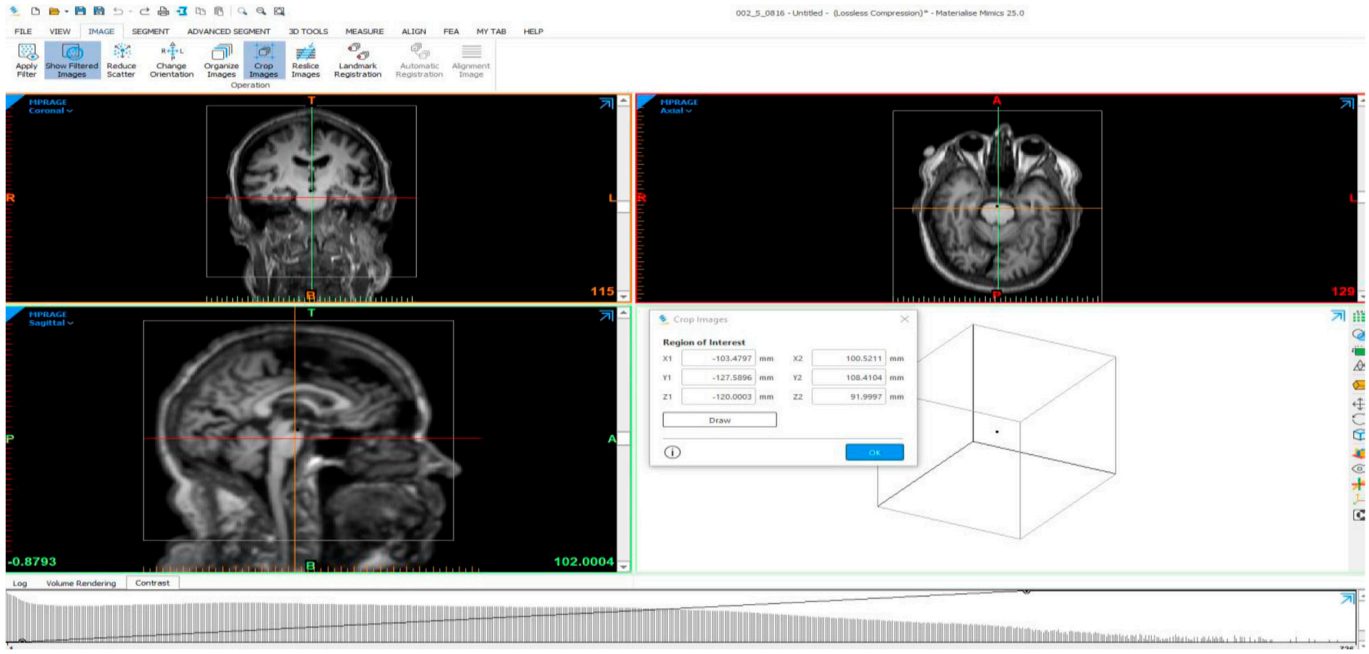

Figure 2. Transformation matrix applied during image cropping illustrating geometric adjustments and spatial alignment.

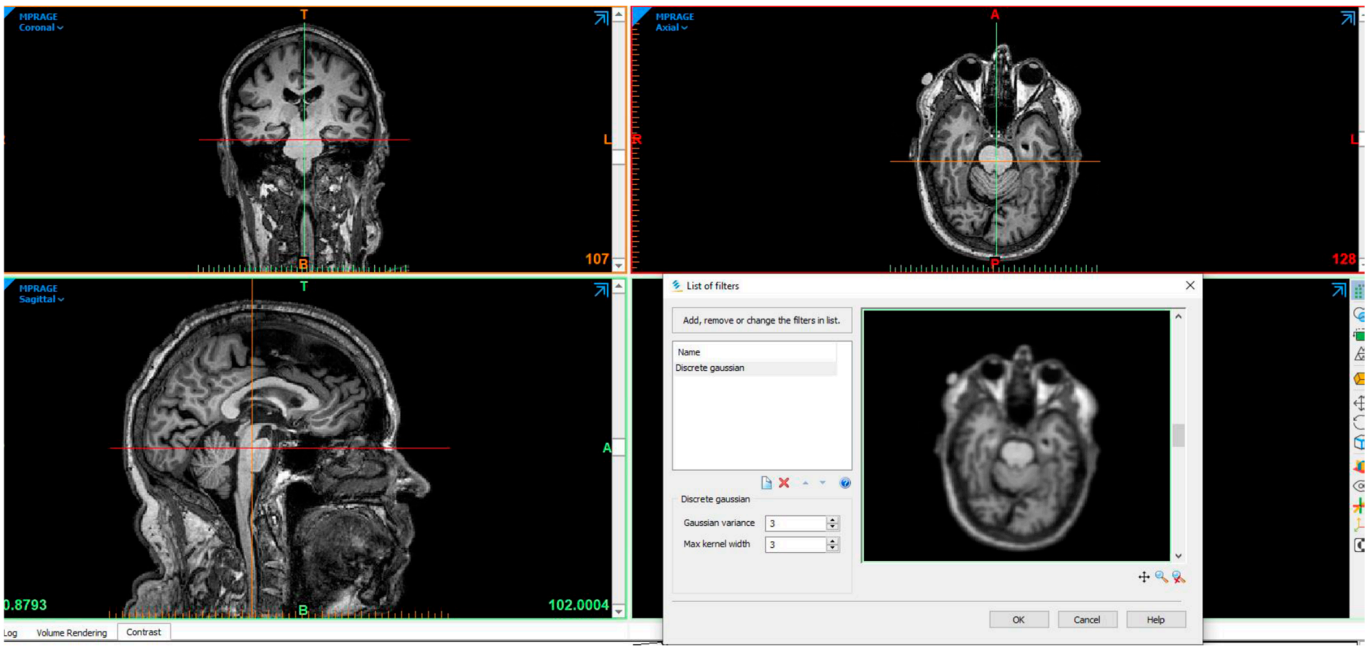

Figure 3. Noise reduction and blurring of non-target areas for enhanced average weighting in desired regions using gaussian filter.

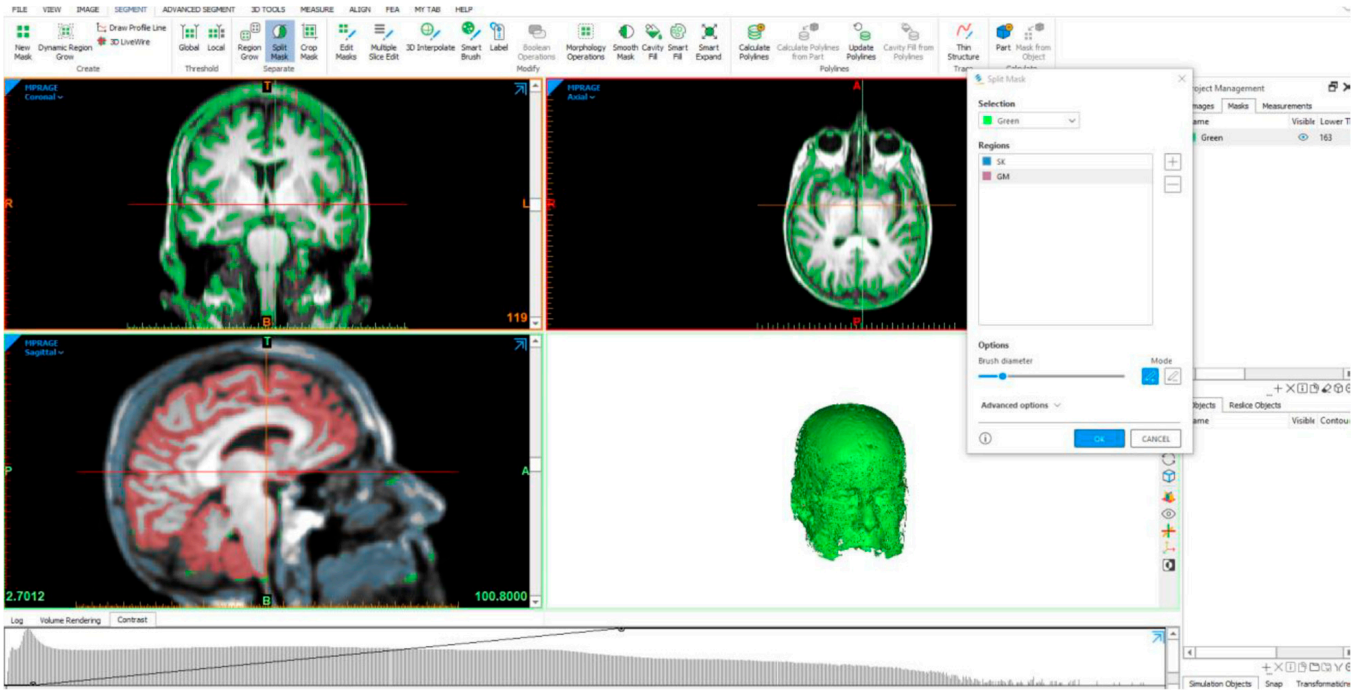

Figure 4. Image segmentation demonstrating voxel value segmentation to distinguish bone, white matter, and gray matter regions.

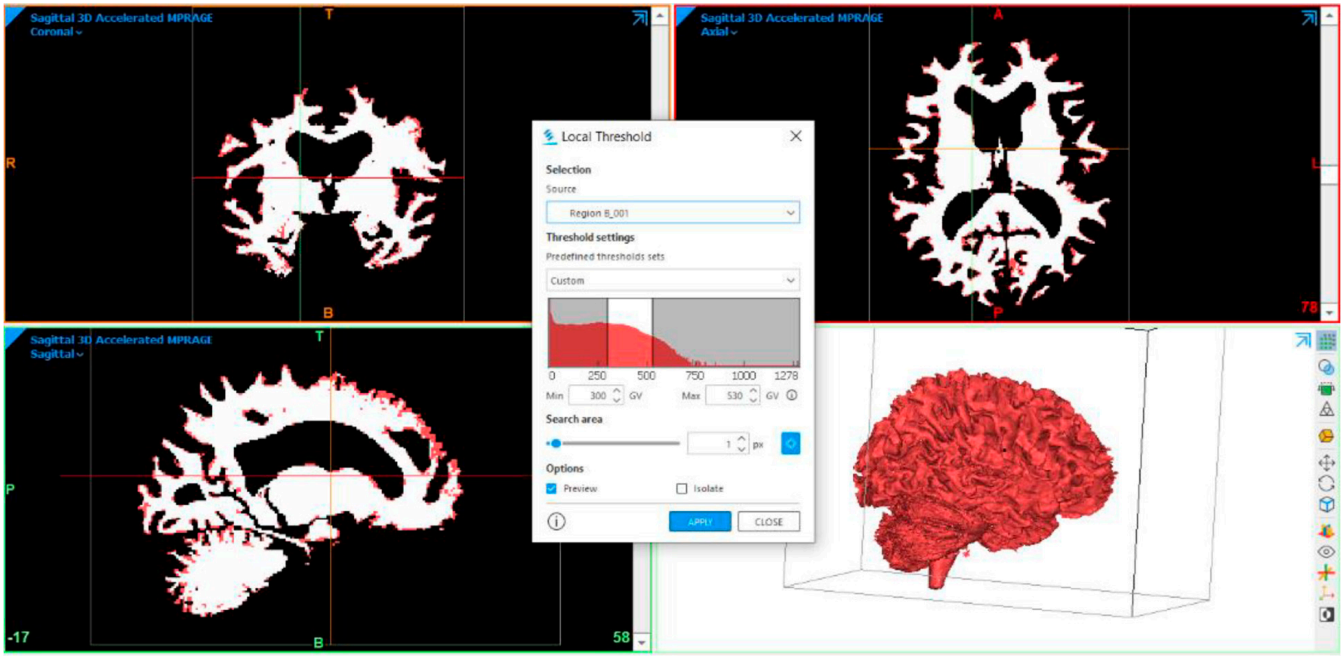

Figure 5. Global thresholding for image segmentation: binary image of white matter and corresponding 3D model representation [16].

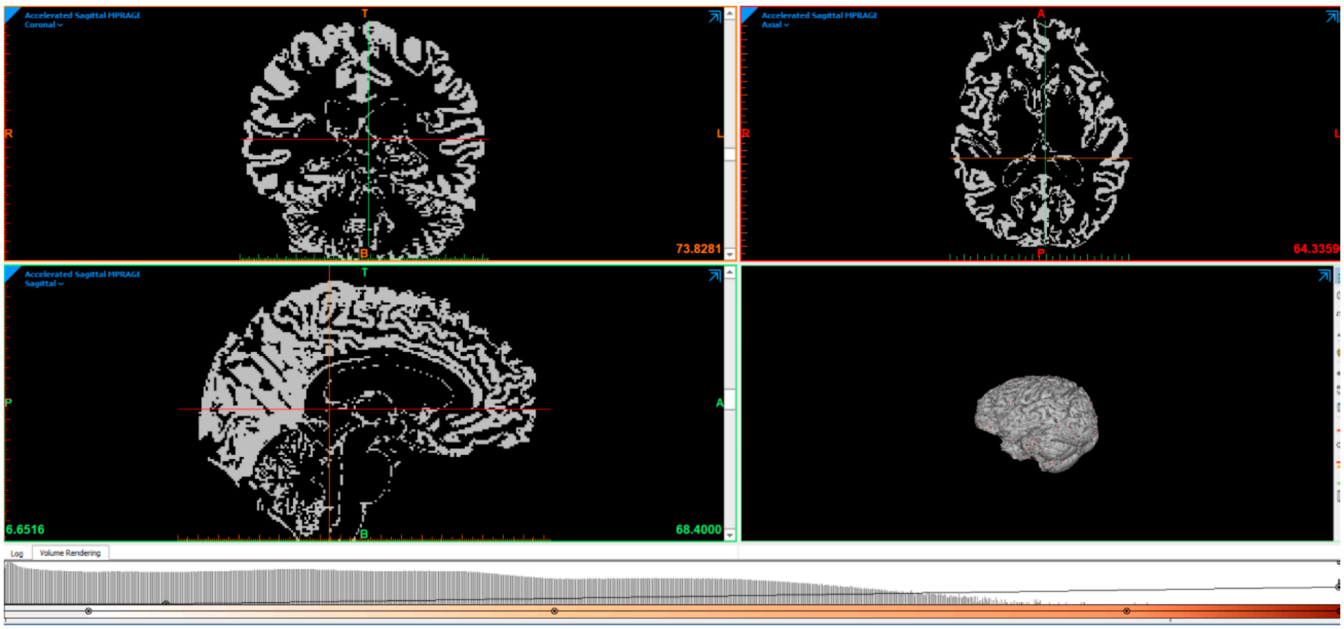

Figure 6. Segmented gray matter image with the corresponding 3D model.

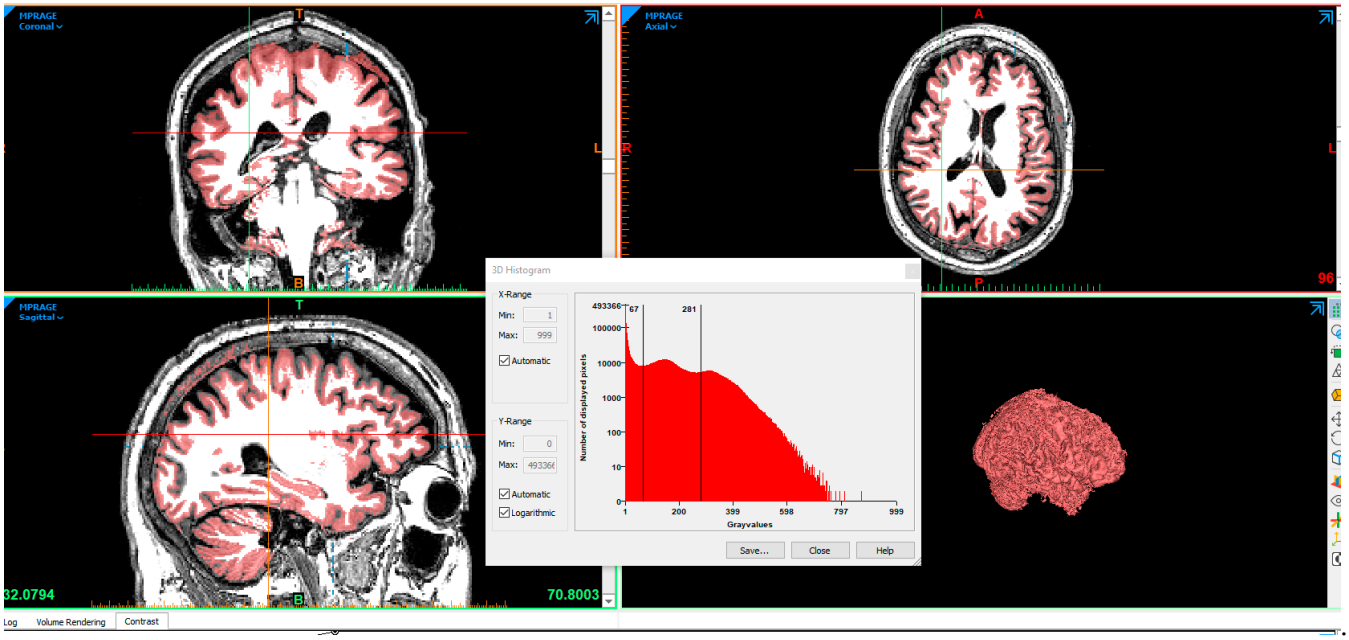

Figure 7. Process workflow for dynamic region—-growing segmentation of gray matter in brain imaging demonstrating 3D histogram analysis and 3D model reconstruction, in a control subject.

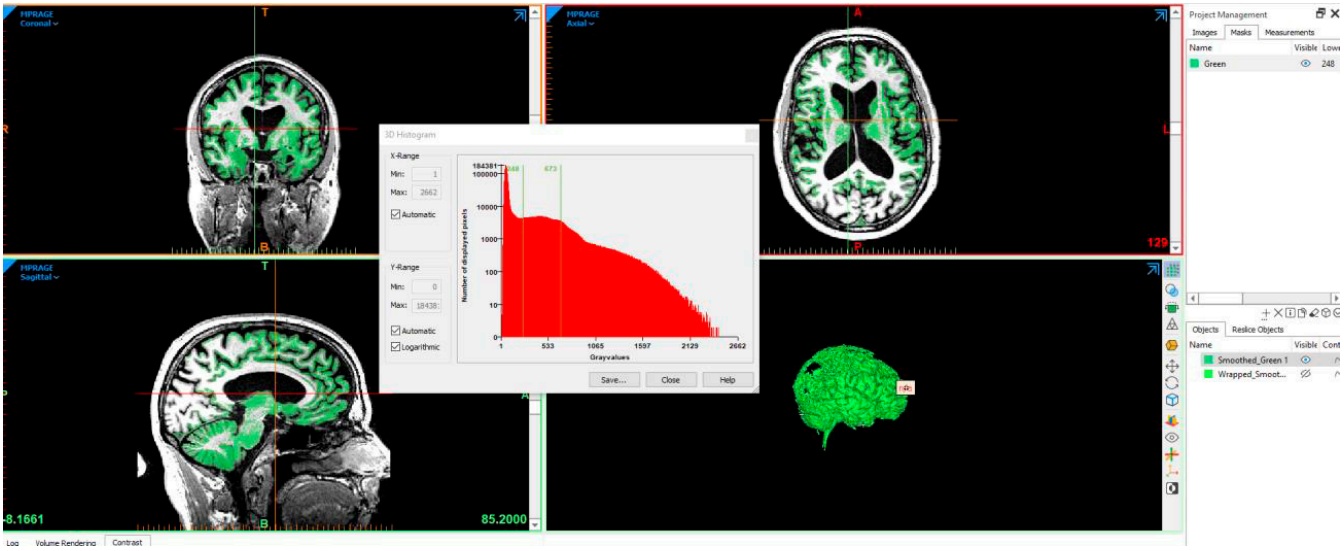

Figure 8. Process workflow for dynamic region—-growing segmentation of gray matter in brain imaging demonstrating 3D histogram analysis and 3D model reconstruction, in an AD subject.

In a simple linear regression, we performed a univariate analysis to compare the association between the gray matter volume of those without AD and those with AD; we found that though the mean part volume of the gray matter in the AD cohort was larger (8.4×10^3 mm^3) compared to the control (4.5×10^3 mm^3) (Table 3), this difference was not statistically different at the 0.05 significance level (p = 0.11) (Figure 10). This may be attributed to the small sample size used in the study and may not be a true representation of the population. Also of importance is the intensity normalization option, which is not available in the current version of the MIMICS software used for voxel morphometric measurements. Intensity inhomogeneity, especially seen in images from high field strength (3T) as used in this study, results in different intensities for the same tissue located differently [17–19]. This may have increased the false positive outcomes in the measurements, which is a major drawback in this study.

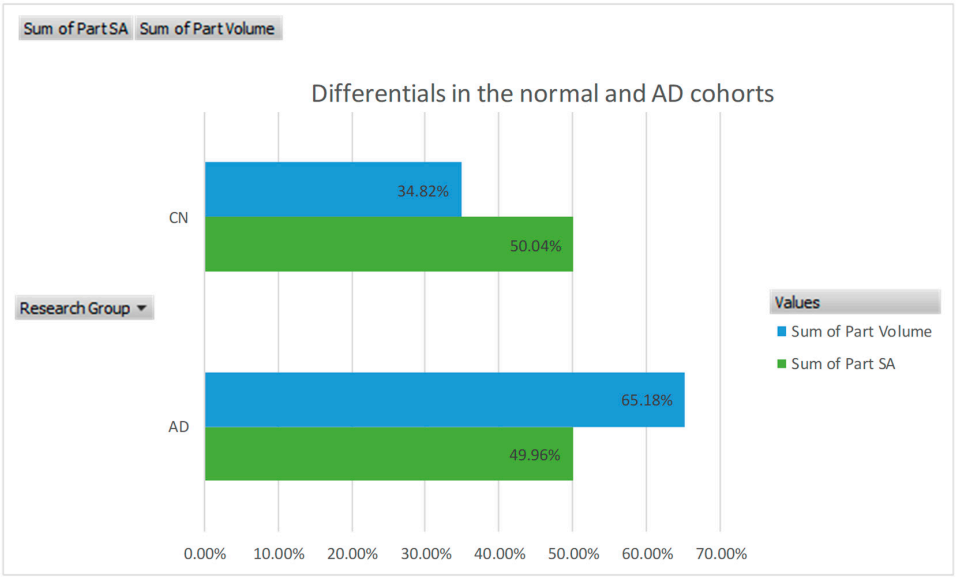

Figure 9. Surface area and volume measurements of brain regions for Alzheimer's disease (AD) and cognitively normal (CN) cohorts.

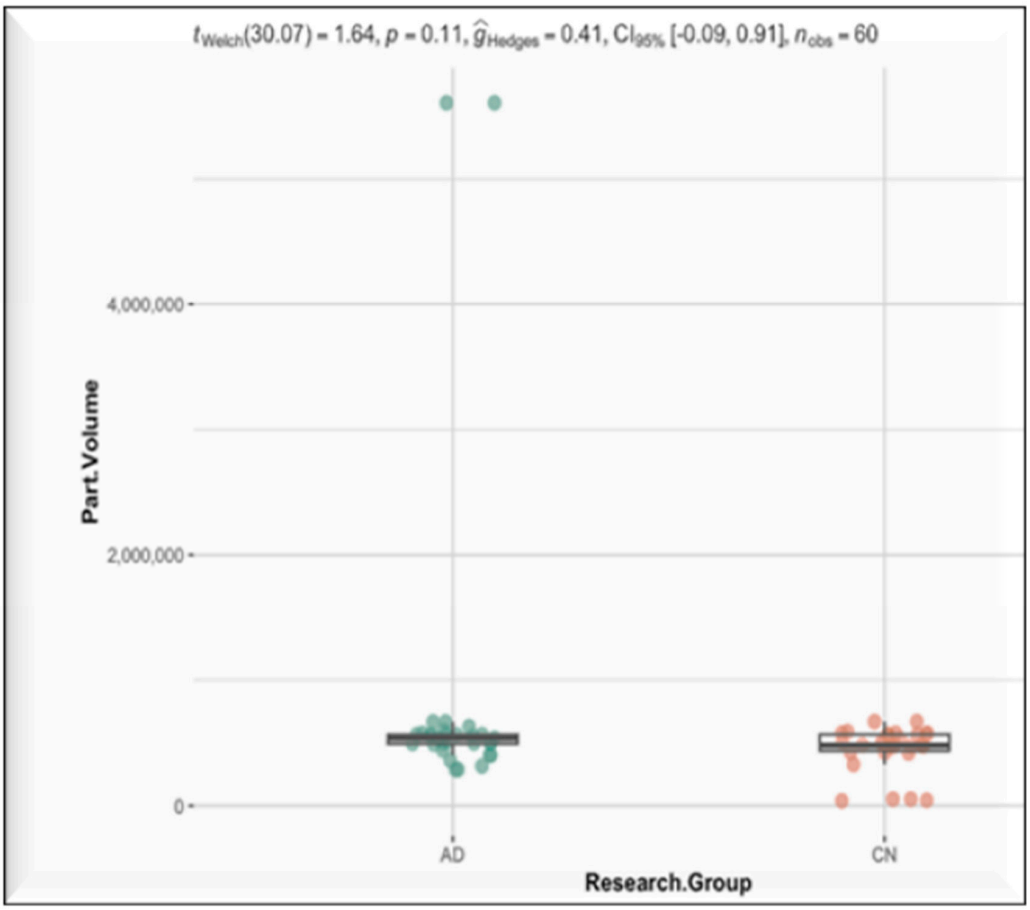

Figure 10. Part volume comparison between research groups.

Table 3. Student's *t*-test results and volume distribution by group.

	Mean	Std. Dev	Min	Median	Max
AD	844,474.97	1,299,250.80	287,200.20	534,701.10	5,610,393.37
CN	451,082.10	176,473.57	38,048.06	480,647.57	667,724.42

3.1. Generic Regression Models

A multivariate logistic regression model was performed that adjusted for part surface area, part volume, age, sex, and weight to check for an association between these factors and the overall risk of developing Alzheimer's disease from the research group under study. We calculated as follows:

Response: research group (Y = 1 or 0).

Predictors: part surface area (X1), part volume (X2), age (X3), sex, (X6) weight (X7).

While the male and female subgroup models showed no significant difference, the generic model showed the log odds of developing Alzheimer's disease to be statistically significant for weight at $p = 0.0171$ and for part volume at $p = 0.0364$ (Figure 11). This result aligns with previous work carried out in AD research [2,20]

Though most previous research has indirectly linked obesity with AD, recent research by McGill University hospital scientists has shown a direct correlation between neurodegeneration and obesity in people with Alzheimer's disease. In their sample of 1300 participants, they compared patients with Alzheimer's disease to control patients, as well as obese to non-obese individuals, and discovered that the pattern of gray matter atrophy in both

groups suggested that losing excess weight could slow the progression of cognitive decline, both in aging and in lowering the risk of AD [20].

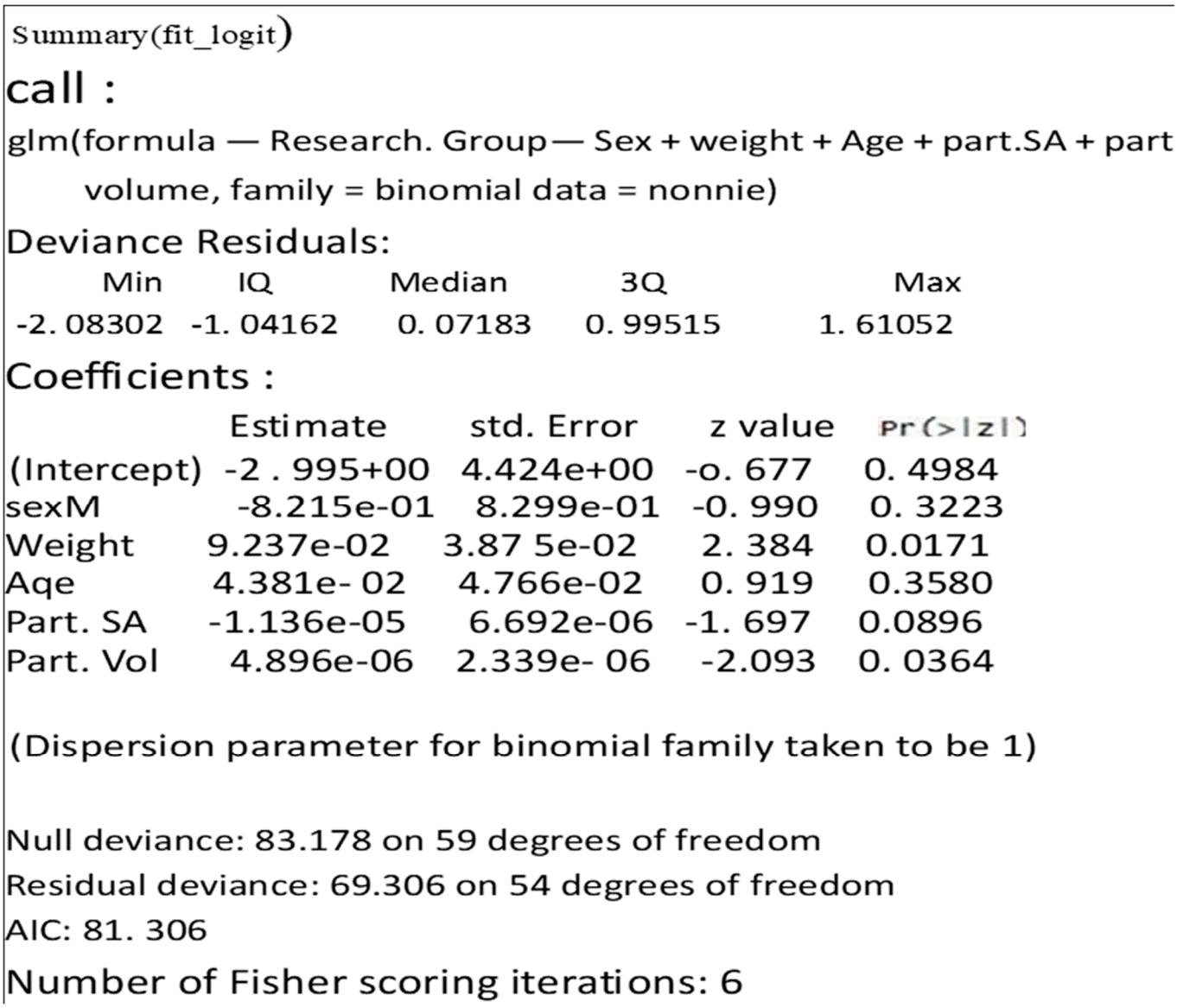

Figure 11. Summary of the generalized model for the research group.

3.2. Part Volume Whole Model

In a comparable regression analysis aimed at correlating part volume measurements between the two groups, adjustments were made for other known variables. For ease of analysis, the age and weight factors were parametrized, as detailed in Table 4. The generic model showed a significant difference at $p = 0.0004$ (Figure 12). However, these effect tests (Table 5) were observed from the gender and age adjustments, which showed a statistically significant difference of $p = 0.0143$ and $p = 0.0019$, respectively. The 65.1–70.1 age group labeled B (Table 4) showed a very statistically significant difference at $p < 0.001$. This result supports previous studies that have reported age to be the greatest of the three risk factors of AD [2,15,21].

Table 4. Age and weight factor categorization and labeling.

Age Factor (Years)	Parameter Label	Weight Factor (kg)	Parameter Label
60.1–65	A	30–40	TA
65.1–70.1	B	40.1–50.1	UB
70.2–75.2	C	50.2–60.2	VC
75.3–80.3	D	60.3–70.3	WD
80.4–85.4	E	70.4–80.4	XE
85.5–90.5	F	80.5–90.5	YF
		90.6–102	ZG

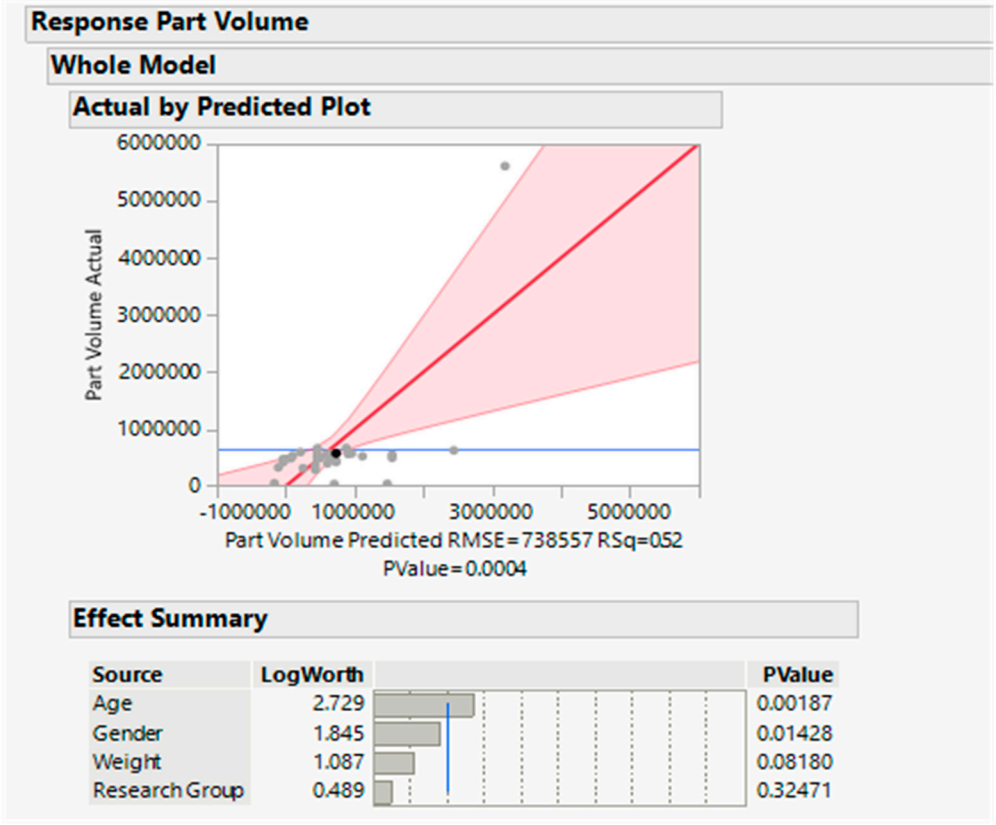

Figure 12. A generic regression model of part volume measurements in Alzheimer's disease (AD) and control groups.

Table 5. Summary of effect tests in the generic model for part volume analysis.

Source	NPam	DF	Sum of Squares	F Ratio	Prob > F
Gender	1	1	3.5383×10^{12}	6.4867	0.0143
Weight	6	6	6.6179×10^{12}	2.0221	0.0818
Research	1	1	5.456×10^{11}	0.9910	0.3247
Age	5	5	1.2417×10^{13}	4.5527	0.0019

3.3. Part Surface Area Whole Model

Conversely, a multivariate logistic regression model was performed with the surface area response variable obtained from MIMICS (Figure 13) that adjusted for age, sex, weight, and gender to check for an association between these factors in both the AD and control groups. The model showed statistical significance at the 0.05 critical level with $p = 0.0111$,

with the age factor accounting for this effect with $p = 0.00750$ (Table 6). This result further affirms the age risk factor in Alzheimer's disease and the potential of MIMICS as a reliable tool despite the limitations.

Table 6. Summary of the effect tests in the surface area model.

Gender	**1**	**1**	**23,049,806.6**	**0.0044**	**0.9477**
Weight	6	6	3.8071×10^{10}	1.1996	0.3236
Research Group	1	1	9,491,869,268	1.7945	0.1870
Age	5	5	9.6028×10^{10}	3.6310	0.0075

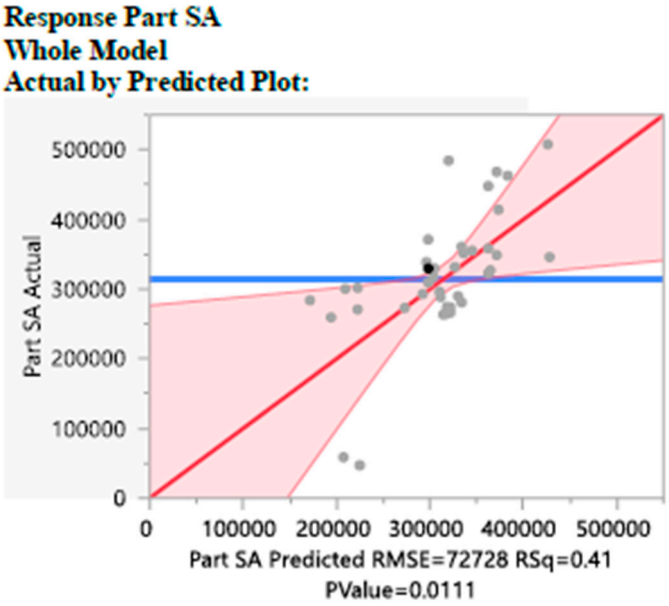

Figure 13. A generic regression model for part surface area measurements in Alzheimer's disease (AD) and control groups.

The bivariate fit of the probability of part volume measurements amongst the female AD cohort showed a sigmoid curve whose summary characteristics' output showed a strong correlation coefficient between the two variables (0.96) (Figure 14). The lower 95% CI for the correlation is 0.956, while the upper confidence interval is 0.971 which means that we are 95% confident that the true correlation coefficient falls between these values. In addition, the significance probability was <0.0001, indicating a statistically significant correlation coefficient, making it unlikely that this observed correlation occurred by chance. Though similar simulations were carried out for males in the control ($N = 11$) and diseased groups ($N = 13$), the skewed data points in the sample of the study showed a comparable probabilistic distribution to be a normal mixture with no significant correlation across them (Figure 14). This could be attributed to the smaller distribution of the male cohort in the sample under study.

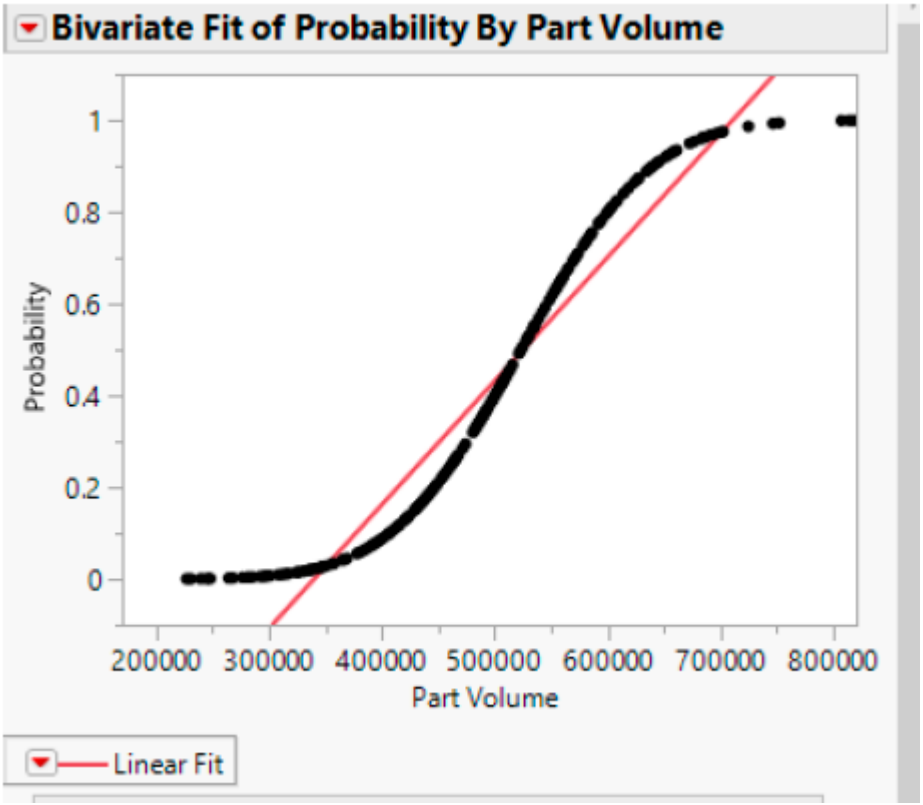

Figure 14. Bivariate analysis of part volume probability for the female Alzheimer's disease (AD) subgroup [16].

4. Conclusions

Based on the results obtained in this research, it may be concluded that MIMICS may be a representative tool for conducting brain morphometry research. This study explored the application of voxel-based morphometry (VBM) using MIMICS software as a potential biomarker for Alzheimer's disease (AD), utilizing MPRAGE T1-weighted MRI data to assess cortical atrophy in a cohort of 60 participants (30 AD patients and 30 controls). Our findings revealed statistically significant differences in cortical volume and surface area between the AD and control groups, with p-values of 0.0004 and 0.011, respectively. Additionally, the impact of age on cortical atrophy was evident, particularly in the 65–70 age group, where the association with AD was most pronounced (p-value < 0.001).

However, while the model demonstrated an accuracy of 0.68, with sensitivity and specificity values of 0.63 and 0.73, respectively, we acknowledge that these metrics indicate the model is still in the early stages of development. This level of accuracy underscores the need for further optimization and validation before the model can be considered for clinical application as a reliable biomarker. The observed correlations, particularly the 96% degree of correlation in female AD participants, are promising but require further exploration to confirm their consistency across larger and more diverse populations.

Future research should focus on improving the automated pipeline within MIMICS to enhance accuracy and reproducibility. Expanding the study population to include a broader spectrum of AD progression and healthy controls will be crucial for increasing the generalizability of our findings. Additionally, integrating multi-modal imaging techniques, such as functional MRI and diffusion tensor imaging, could provide a more comprehensive validation of MIMICS and further establish its utility in AD research. While our study offers initial insights, it serves as a foundation for further investigation and development in this promising area of research.

Author Contributions: Conceptualization, T.G.; Methodology, N.A.; Software, N.A.; Validation, N.A.; Investigation, N.A.; Resources, T.G.; Writing—original draft, N.A.; Writing—review & editing, T.G.; Supervision, T.G. All authors have read and agreed to the published version of the manuscript.

Funding: This research received no external funding.

Data Availability Statement: The data that support the findings of this study are openly available in ADNI upon request at (https://adni.loni.usc.edu).

Conflicts of Interest: The authors declare no conflict of interest.

References

1. 2024 Alzheimer's disease facts and figures. *Alzheimers Dement.* **2024**, *20*, 3708–3821. [CrossRef] [PubMed] [PubMed Central]
2. Jack, C.R., Jr.; Knopman, D.S.; Jagust, W.J.; Shaw, L.M.; Aisen, P.S.; Weiner, M.W.; Petersen, R.C.; Trojanowski, J.Q. Hypothetical model of dynamic biomarkers of the Alzheimer's pathological cascade. *Lancet Neurol.* **2010**, *9*, 119–128. [CrossRef] [PubMed] [PubMed Central]
3. Chow, N.; Hwang, K.S.; Hurtz, S.; Green, A.E.; Somme, J.H.; Thompson, P.M.; Elashoff, D.A.; Jack, C.R.; Weiner, M.; Apostolova, L.G.; et al. Comparing 3T and 1.5T MRI for mapping hippocampal atrophy in the Alzheimer's Disease Neuroimaging Initiative. *AJNR Am. J. Neuroradiol.* **2015**, *36*, 653–660. [CrossRef] [PubMed] [PubMed Central]
4. Villemagne, V.L.; Burnham, S.; Bourgeat, P.; Brown, B.; Ellis, K.A.; Salvado, O.; Szoeke, C.; Macaulay, S.L.; Martins, R.; Maruff, P.; et al. Amyloid β deposition, neurodegeneration, and cognitive decline in sporadic Alzheimer's disease: A prospective cohort study. *Lancet Neurol.* **2013**, *12*, 357–367. [CrossRef] [PubMed]
5. Vemuri, P.; Jack, C.R. Role of structural MRI in Alzheimer's disease. *Alzheimer's Res. Ther.* **2010**, *2*, 23. [CrossRef]
6. Rajan, K.B.; Weuve, J.; Barnes, L.L.; McAninch, E.A.; Wilson, R.S.; Evans, D.A. Population estimate of people with clinical Alzheimer's disease and mild cognitive impairment in the United States (2020–2060). *Alzheimer's Dement.* **2021**, *17*, 1966–1975. [CrossRef] [PubMed] [PubMed Central]
7. Rao, Y.L.; Ganaraja, B.; Murlimanju, B.V.; Joy, T.; Krishnamurthy, A.; Agrawal, A. Hippocampus and its involvement in Alzheimer's disease: A review. *3 Biotech* **2022**, *12*, 55. [CrossRef] [PubMed] [PubMed Central]
8. Wu, J.; Shahid, S.S.; Lin, Q.; Hone-Blanchet, A.; Smith, J.L.; Risk, B.B.; Bisht, A.S.; Loring, D.W.; Goldstein, F.C.; Levey, A.I.; et al. Multimodal magnetic resonance imaging reveals distinct sensitivity of hippocampal subfields in asymptomatic stage of Alzheimer's disease. *Front Aging Neurosci.* **2022**, *14*, 901140. [CrossRef] [PubMed]
9. Ho, A.J.; Hua, X.; Lee, S.; Leow, A.D.; Yanovsky, I.; Gutman, B.; Dinov, I.D.; Leporé, N.; Stein, J.L.; Toga, A.W.; et al. Comparing 3 T and 1.5 T MRI for tracking Alzheimer's disease progression with tensor-based morphometry. *Hum. Brain Mapp.* **2010**, *31*, 499–514. [CrossRef] [PubMed] [PubMed Central]
10. Xu, J.Q.; Murphy, S.L.; Kochanek, K.D.; Arias, E. *Mortality in the United States, 2021*; NCHS Data Brief, no 456; National Center for Health Statistics: Hyattsville, MD, USA, 2022. [CrossRef]
11. Weiner, M.W.; Veitch, D.P.; Aisen, P.S.; Beckett, L.A.; Cairns, N.J.; Green, R.C.; Harvey, D.; Jack, C.R., Jr.; Jagust, W.; Morris, J.C.; et al. The Alzheimer's Disease Neuroimaging Initiative 3: Continued innovation for clinical trial improvement. *Alzheimer's Dement.* **2017**, *13*, 561–571. [CrossRef] [PubMed] [PubMed Central]
12. Silbert, L.C.; Quinn, J.F.; Moore, M.M.; Corbridge, E.; Ball, M.J.; Murdoch, G.; Sexton, G.; Kaye, J.A. Changes in premorbid brain volume predict Alzheimer'sdisease pathology. *Neurology* **2003**, *61*, 487–492. [CrossRef]
13. Pagnozzi, A.M.; Fripp, J.; Rose, S.E. Quantifying deep gray matter atrophy using automated segmentation approaches: A systematic review of structural MRI studies. *Neuroimage* **2019**, *201*, 116018. [CrossRef] [PubMed]
14. Ashburner, J.; Friston, K.J. Why voxel-based morphometry should be used. *Neuroimage* **2001**, *14*, 1238–1243. [CrossRef]
15. Testa, C.; Laakso, M.P.; Sabattoli, F.; Rossi, R.; Beltramello, A.; Soininen, H.; Frisoni, G.B. A comparison between the accuracy of voxel-based morphometry and hippocampal volumetry in Alzheimer's disease. *J. Magn. Reason. Imaging* **2004**, *19*, 274–282. [CrossRef] [PubMed]
16. Aniebo, N.B. Brain Morphometry from Neuroimaging as a Biomarker For Alzheimer's Disease. Master's Thesis, OhioLINK Electronic Theses and Dissertations Center, Wright State University, Dayton, OH, USA, 2023. Available online: http://rave.ohiolink.edu/etdc/view?acc_num=wright1685447122622787 (accessed on 1 December 2023).
17. Nemoto, K. Understanding Voxel-Based Morphometry. *Brain Nerve* **2017**, *69*, 505–511. (In Japanese) [CrossRef] [PubMed]
18. Hirata, Y.; Matsuda, H.; Nemoto, K.; Ohnishi, T.; Hirao, K.; Yamashita, F.; Asada, T.; Iwabuchi, S.; Samejima, H. Voxel-based morphometry to discriminate early Alzheimer's disease from controls. *Neurosci. Lett.* **2005**, *382*, 269–274. [CrossRef]
19. Goto, M.; Abe, O.; Hagiwara, A.; Fujita, S.; Kamagata, K.; Hori, M.; Aoki, S.; Osada, T.; Konishi, S.; Masutani, Y.; et al. Advantages of Using Both Voxel- and Surface-based Morphometry in Cortical Morphology Analysis: A Review of Various Applications. *Magn. Reson. Med. Sci.* **2022**, *21*, 41–57. [CrossRef]

20. McGill University. Study Finds Obesity-Related Neurodegeneration Mimics Alzheimer's Disease: Controlling Excess Weight Could Lead to Improved Health Outcomes, Slow Cognitive Decline. ScienceDaily. (31 January 2023). Available online: www.sciencedaily.com/releases/2023/01/230131101852.htm (accessed on 23 April 2023).
21. Ahburner, J.; Friston, K.J. Voxel-based morphometry--the methods. *Neuroimage* **2000**, *11*, 805–821. [CrossRef] [PubMed]